Chapter 5
Stimulus Localization by Neuronal Populations in Early Visual Cortex: Linking Functional Architecture to Perception

Dirk Jancke, Fréderic Chavane, and Amiram Grinvald

Abstract In primary visual areas any local input is initially transmitted via horizontal connections giving rise to a transient peak of activity with spreading surround. How does this scenario change when the stimulus starts to move? Psychophysical experiments indicate that localization is different for stationary flashed and moving objects depending on the stimulus history. We here demonstrate how successively presented stimuli alter cortical activation dynamics. By a combination of electrophysiological and optical recordings using voltage-sensitive dye we arrive at the conclusion that sub-threshold propagating activity pre-activates cortical regions far ahead of thalamic input. Such an anticipatory mechanism may contribute in shifts of the perceived position as observed for the flash-lag effect and line-motion illusion in human psychophysics.

5.1 Introduction

How are local stimuli represented across primary visual cortex? Even small visual objects activate large populations of neurons that form extended and densely interconnected excitatory and inhibitory circuits acting on millisecond time scales. The dynamic balance between these antagonist circuits thereby determines each cells' output and hence the amount of information being transmitted further downstream to form perceptual events.

In this chapter we review how the primary visual cortex represents position of small stimuli that are briefly flashed or moved. Neuronal representations of appearing visual objects, the sudden onset of motion, or tracking of moving objects are necessarily confronted with the need of processing accurately space and time. Localization of visual objects must therefore deal with neuronal delays.

We further address the question in, how far activity in early cortical areas correlates to visual perception without the need of top-down contributions due to

D. Jancke (✉)
Department of Neurobiology, Ruhr-University Bochum, ND7/72, Bochum, 44780, Germany
e-mail: jancke@neurobiologie.rub.de

U.J. Ilg and G.S. Masson (eds.), *Dynamics of Visual Motion Processing: Neuronal, Behavioral, and Computational Approaches*,
DOI 10.1007/978-1-4419-0781-3_5,

voluntary action. In particular we focus on well-known visual illusions (flash-lag, line-motion) that are assumed to involve early cortical mechanisms in motion processing. The reported experiments are based on measurements in visual areas 17 and 18 in anaesthetized and paralyzed preparations. Thus the obtained data reflect "automatic" cortical computation without involvement of attentional processes.

Within our framework we link neuronal signals derived from extracellular and voltage-sensitive dye recordings to psychophysical phenomena in order to unravel the relationship between architecture and function of early visual cortex.

5.2 Neuronal Population Dynamics in Visual Space

A small local stimulus evokes widespread cortical activity recruiting thousands of densely interconnected neurons through horizontal connectivity. Figure 5.1 sketches a snapshot of synaptic activity in response to a flashed square measured by voltage-sensitive dye imaging. The fluorescent dye signal reports net neuronal depolarization across the cortical surface, with emphasis on superficial layers. By definition, single neurons fire action potentials more strongly when activated within their receptive field centers (Fig. 5.1, red circles). In contrast, neurons that are stimulated outside their receptive field (RF) may receive input by long-range horizontal connections but do not reach firing thresholds (lower trace Fig. 5.1b).

5.2.1 The Concept of a Population Receptive Field

Taking into account that many neurons with overlapping RFs, are activated when a small stimulus is presented (Fig. 5.1c), we applied a population approach derived from single unit recordings. In this approach, each neuron participates

Fig. 5.1 (continued) (see symbolized spike traces) but are activated subthreshold due to long-range horizontal synaptic input. (**c**) Many neurons with densely overlapping receptive fields (RFs) are stimulated when a small square is presented (colored ellipses sketch their projection in visual field coordinates). (**d**) Time resolved population representation of a square that was flashed in the middle axis of the sampled space. Activity builds-up coherently ~30 ms after stimulus onset, reaches its maximum after ~50 ms, and decays homogenously centered on stimulus location. (**e**) Seven squares within a fixed reference frame (*white outline*) were presented independently of the neurons' individual RF location. Distributions of activity were obtained by pooling the spiking responses of 178 neurons (recordings in cat area 17). Each cell's normalized firing rate in response to the stimuli was mapped to individual RF-centers, resulting in distributions of activity. The responses were interpolated with a Gaussian, with Sigma matching the average RF widths. In summary, each neuron contributes to the entire population activity by its firing rate dependent on the location of its RF-center relative to the stimulus. Time averages of 30–80 ms after stimulus onset are shown (flash duration 25 ms). Note that the peaks of activity are closely around each of the stimulus positions. Thus the applied population approach enables sampling of visual space smaller than average RF sizes (size of squares was 0.4°). (**f**) Population representations derived by means of OLE for all seven elementary stimuli used (time average, 30–80 ms). The optimization procedure allowed the individual peaks to be accurately aligned with the position of each stimulus (*see Color Plates*)

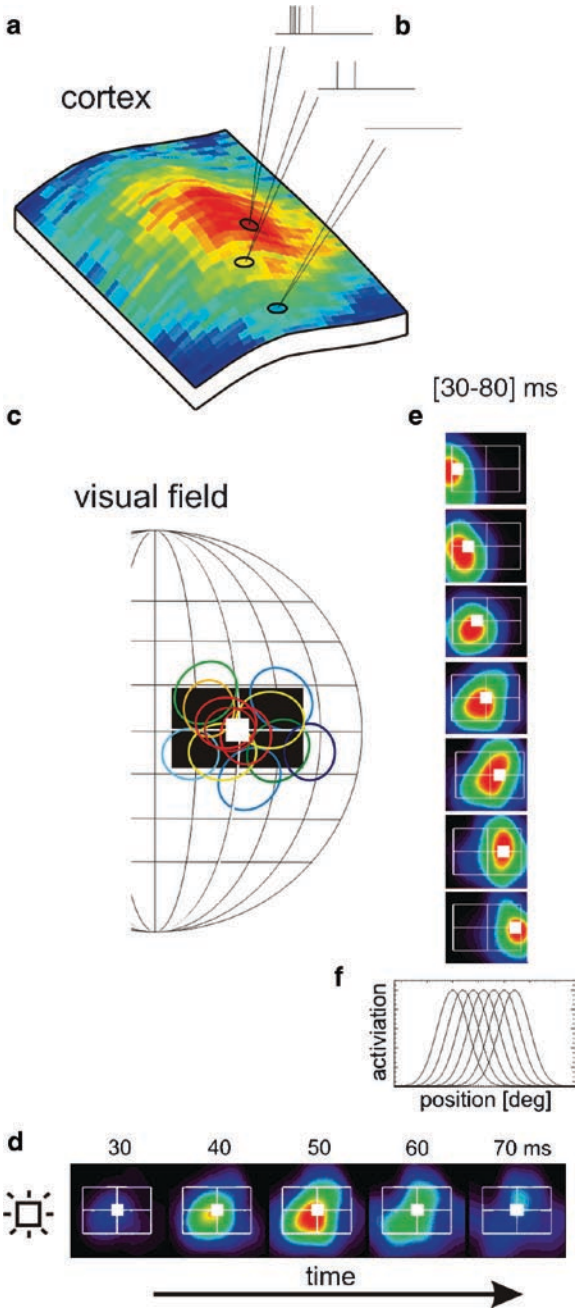

Fig. 5.1 Widespread cortical activity in response to small local stimuli. (**a**) A portion of visual cortex is sketched overlaid with an activity pattern that was evoked by a flashed square. Warm colors indicate high-amplitude activity revealed by voltage-sensitive dye imaging. (**b**) Extracellular measurements at three different recordings sites lead to different results: Whereas neurons that are located around the center of activation reach spiking thresholds, neurons further away do not

in a reconstructed population activity built within a fixed reference frame, here a visual position. Thus, all neurons contribute to the population representation in visual space coordinates dependent on their firing rates and relative RF positions (Jancke et al. 1999, 2004b; Jancke 2000).

Our concept is a straightforward consequence of the observation that a large number of differently tuned neurons are activated, after even the simplest form of sensory stimulation or motor output. For any stimulation, some of these neurons are optimally activated, but the majority sub-optimally, having receptive fields positioned along the edges of a local visual stimulus; for example Fig. 5.1a, c. In addition, under natural viewing conditions stimuli are arbitrarily distributed across many RFs with highly diverse spatio-temporal properties (Szulborski and Palmer 1990; Gegenfurtner and Hawken 1996; Fitzpatrick 2000; Dinse and Jancke 2001a, b; for a similar approach in the somatosensory system see Nicolelis et al. 1998).

5.2.2 *RF-Derived Population Representations of Stimulus Position*

We first applied a straightforward interpolation procedure in which each cell "votes" with its firing rate for the center of its RF into the population code. Each cells' RF center was quantitatively assessed, the resulting RF-profiles were smoothed, and the RF-centers were defined at the location of maximal amplitude.

Subsequently, seven squares were flashed within a fixed reference frame (Fig. 1c, gray area; Fig. 5.1d, e, white rectangle) regardless of the respective RF position, and the cell responses to these stimuli were normalized to the maximum. Thus each cell's normalized response to a given square fed the population representation at their RF-center position. Population responses were then smoothed with a Gaussian (width = 0.6°). The built-up and decay of the population response of 178 neurons is presented in Fig. 5.1d in response to a central stimulation, showing a gradual and well-localized peak of activity centered on the position of the given square (each frame depicts a 10 ms time step).

Time averages of population representations of the seven flashed stimuli are depicted in Fig. 5.1e (white squares). The individual distributions of activity in response to squares at different locations can be regarded as the summed activity profile within a population's receptive field (PRF[1]). The extent of the PRF is larger than the retinotopic stimulus representation, and reflects the average RF size and scatter in cat area 17 (Albus 1975). However, our population procedure allows reconstruction of stimulus position in resolutions much smaller than individual RF sizes.

[1] We used this term for spiking distributions of population activity (Jancke et al. 1999, 2004b). Originally, the term was introduced for LFP recordings (Victor et al. 1994), and most recently applied for voxel analysis of fMRI data (Dumoulin and Wandell 2008).

5.2.3 OLE-Derived Population Representations of Stimulus Position

As an alternative to the RF-derived interpolation procedure, and in order to construct the PRF in a well defined mathematical way, we employed an Optimal Linear Estimator (OLE). This technique, originally developed to estimate a single value of an encoded physical quantity (Salinas and Abbott 1994), is based on a Bayesian theoretical framework (Dayan and Abbott 2001). We used an extension of this method that enabled us to estimate entire distributions of population activity across visual space (Jancke et al. 1999, 2004b; Jancke 2000; Jazayeri and Movshon 2006).

The method is based on two ideas. First, the population distribution is generated as a linear superposition of a set of basis functions, one such function for each neuron. Each neuron's basis function is multiplied with the current firing rate of the neuron. Second, a template function for the distribution of population activity was defined as a Gaussian centered at each of the seven reference stimulus positions. Its width (0.6°) in visual space approximately matched the average RF profile of all neurons measured (Jancke et al. 1999). The basis function of each neuron was determined such that for the seven reference stimuli the reconstructed population distribution approximated the template function optimally. For this optimization, we used the mean firing rates within the time interval around maximum activity, 40–65 ms after the onset of the stimulus. However, the exact size of the integration window was not critical for the estimation procedure.

Figure 5.1f depicts distributions of population activity in the specified time window with high precision in visual space. Note that all seven flashes were fairly represented by 0.4° shifts of activity profiles across the PRF. This reconstruction was used as a tool for the next step, the calculation of motion trajectories across the PRF.

5.2.4 Representation of Moving Stimuli across the PRF

To extend the estimation to moving stimuli, the basis function that each neuron contributes to the seven reference stimuli was held fixed, but was now multiplied with the firing rate of that neuron in response to a stimulus moving with a particular velocity.

For all speeds and both directions tested, Fig. 5.2 depict space-time diagrams of OLE-derived population distributions within the time intervals that revealed significant propagation of spiking activity. The diagrams show coherent peaks of activity tracking each moving stimulus across the PRF. Dependent on speed we observed a spatial lag between the current stimulus position and the activity peaks (compare Fig. 5.4), which were most evident at high stimulus speeds (see red and blue lines). The profiles of the PRF showed some variability in response amplitudes and scatter

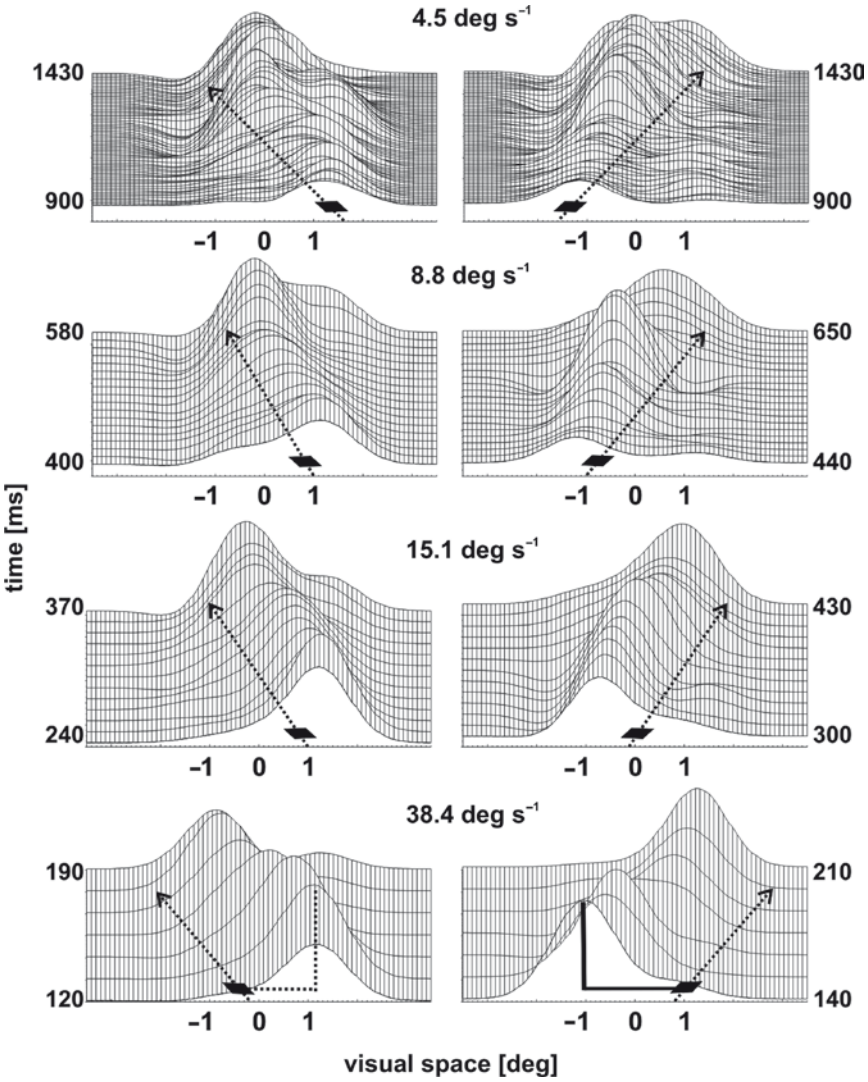

Fig. 5.2 Motion trajectories across the population receptive field (PRF). Space-time diagrams of population activity representing squares that moved with different speeds and directions (stimulus shown in *black*, *arrows* sketch trajectories). Profiles were derived by OLE. The *x*-axis depicts visual space in degree, zero indicating mid-point of trajectories. Starting position of movement was at ±3.2°. *Left column* shows propagation reflecting peripheral-central motion; *right column* shows opposite direction. The *y*-axis resolves 10 ms time steps within the time interval in which propagation of activity occurred. Activity was normalized for each speed separately. The different tilt angles of the space-time plots arise from activity peaks matching stimulus speed and direction. *Red and blue lines* in the *bottom row* sketch the spatial lag between current stimulus position and peak location within the PRF (cf. Fig. 5.4). (Modified from Jancke et al. ©2004b, by permission from Wiley-Blackwell)

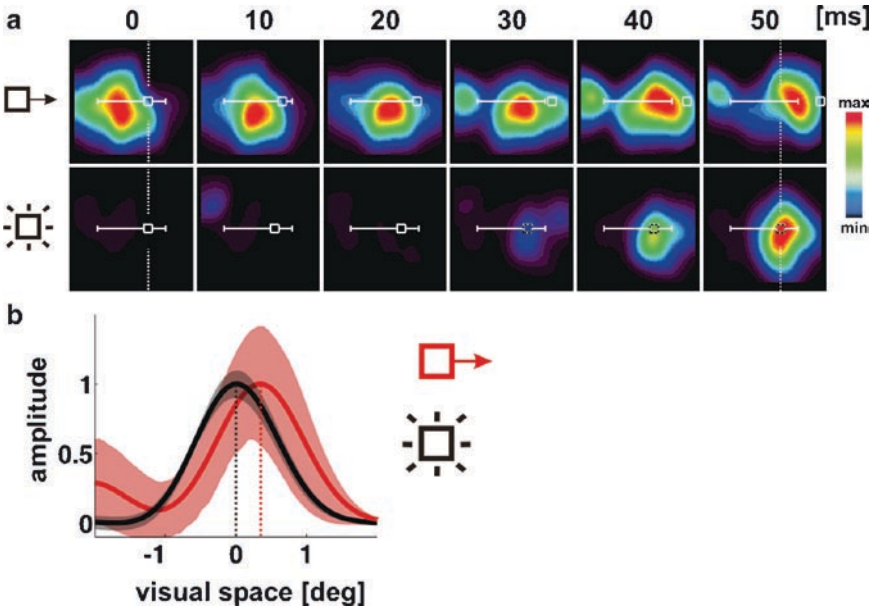

Fig. 5.3 The flash lags: impact of shorter latency for motion compared to a flash on the representation of position. (**a**) *Upper row*: moving square (38.4°s^{-1}). *Lower row*: flashed square (outlined in white; 25 ms on; shown stippled after stimulus off). Population representations are shown in time frames of 10 ms from *left* to *right*. The sampled space covered 2.8° of the central visual field (*horizontal white line*, cf. Fig. 5.1). *Color bar* indicates level of population activity; data were normalized separately for each stimulus condition. The moving stimulus started 3.2° outside the sampled visual space tracked by a peak of population activity that has been evoked some time before beyond the sampling region. At time zero stimulus position was identical for the moving and the flashed square (compare *vertical pointed lines*). During the next time steps activity in response to the flash emerged while the moving peak continued propagating. When activity for the flashed stimulus reached its maximum (50 ms), the moving peak already passed the mutual flash position due to its faster processing. (**b**) The spatial offset shown in (**a**) was confirmed applying the OLE approach in combination with a bootstrap analysis ($n = 1{,}000$). The time window shown depicts activity 50–60 ms after presentation of the flashed stimulus. Activity was separately normalized to the mean of each stimulus condition. *Gray shaded* areas show 99% confidence intervals for the flashed stimulus (*bright gray*; *black line* shows mean), respectively for the moving square (*bright red*; *red line* shows mean). A clear spatial offset ($p < 0.00001$) can be seen between the peaks of both conditions due to reduced time-to-peak latencies in response to motion (*vertical dotted line*).(Modified from Jancke et al. ©2004b, by permission from Wiley-Blackwell) (*see Color Plates*)

in peak positions. These fluctuations were due to irregularities in cell sampling and of no significance ($p > 0.05$, bootstrap, $n = 1{,}000$). Thus, our approach depicts propagating population activity on a fine spatial scale, resolving shifts of activity peaks in visual space much smaller than the RF sizes (see Fig. 5.3a upper row, for a motion trajectory derived from the RF interpolation procedure).

5.2.5 *The Flash-Lag Effect: Differences between Flashed and Moving Stimuli*

Judging correctly the location of moving objects is of crucial importance for evading obstacles or predators or for catching prey. This task would be almost impossible, particularly for high speeds, if the relevant information is delayed due to neural conduction and processing times. To overcome this problem, compensatory mechanisms have evolved that allow for anticipation of the path of motion.

Psychophysically, a moving and a flashed stimulus presented aligned, are perceived as being displaced: Surprisingly, the moving stimulus appears ahead of the flash (Hazelhoff and Wiersma 1924). One explanation for this "flash-lag" effect is that the visual system is predictive and extrapolates the position of a moving stimulus into the future (Nijhawan 1994). Alternatively, the "latency difference" model assumes that the visual system processes moving objects more rapidly compared to single flashes (Purushothaman et al. 1999; Kirschfeld and Kammer 1999; Whitney et al. 2000; for review and other explanations see Eagleman and Sejnowski 2000; Krekelberg and Lappe 2001). In none of those studies, however, were neurophysiological correlates examined. We therefore used our population approach for comparison between population representations of a single flash and a moving square.

The upper row in Fig. 5.3a illustrates the central portion of a motion trajectory of a square moving at a speed of 38.4°s^{-1}. At the onset of the flash (lower row, time zero), the moving square is located at the same position as the flashed square. Clearly, due to neural delay times, cortical population activity for the flash at that time is at baseline. In contrast, for the moving square, a propagating peak of activity is already observed that had been evoked previously since the stimulus trajectory started outside the PRF (see supplementary movie 1). Five steps later (50 ms), the moving stimulus is at a new position, tracked by the peak of population activity with a spatial lag. At that time, activity for the flash has reached its maximum without changing position, thus representing faithfully the initial location of the stimulus. Applying the OLE procedure, Fig. 5.3b depicts the same situation as shown in Fig. 5.3a, 50 ms, after presentation of the flash. We found the peak representing the moving stimulus approximately 0.33° ahead of the peak representing the flash.

5.2.6 *Latency Differences – Spatial Offset – Directional Asymmetry*

Assuming equal processing times for both flashed and moving stimuli, the population representations should be localized at identical positions. Instead, activity peaks elicited by motion and the flash showed a significant spatial offset, i.e. the moving square was represented ahead of the flash, indicating shorter latencies for motion due to the past history created by the moving stimulus.

To compare latencies evoked by single flashes with those for moving stimuli, we used the spatial lag method introduced by Bishop et al. (1971) for analysis of single cell latencies. This method is based on the fact that the time-to-peak of activity depends on stimulus speed. As our approach, produces continuous propagation of activity across the PRF (Figs. 5.2 and 3a) rather than single discharge peaks we modified the original method: Along the entire trajectory across the PRF, we calculated the average spatial lag between current stimulus position and its representing activity peak. This mean spatial lag was plotted as a function of stimulus speed (Fig. 5.4) indicating that the spatial lag increased linearly with stimulus speeds.

The slope of the regressions revealed latencies of 38 ms for the peripheral-central ($r=0.99$) and 42 ms ($r=0.99$) for central-peripheral direction. The spatial lag was significantly shorter than estimated from time-to-peak latencies in response to flashed stimulation (~54 ms, mean peak latency for single flashes across the PRF; bootstrap).

The spatial lag was also dependent on the direction of motion. Peripheral-central movement's latencies were smaller compared to the opposite direction, particularly for higher speeds (see Fig. 5.2). With decreasing speed, this asymmetry became less significant due to the increasing positional scatter ($p<0.01$ for $8.8°s^{-1}$; $p>0.05$ for $4.5°s^{-1}$). For a slow speed of $4.5°s^{-1}$, reduced latency for peripheral-central motion

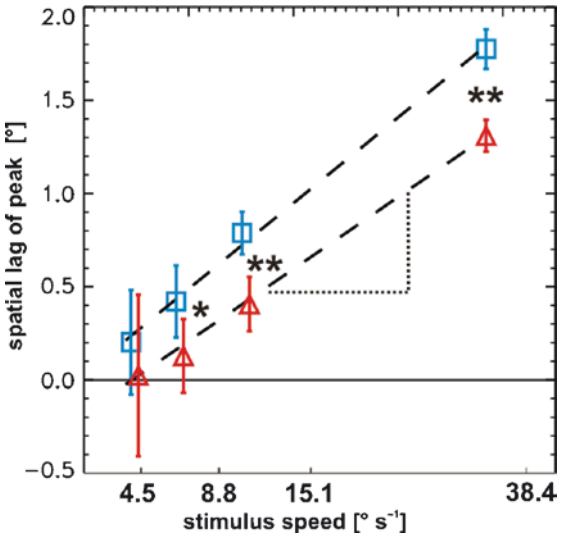

Fig. 5.4 Calculation of peak latencies for moving stimuli: speed-dependence of the spatial lag. The average spatial lag between the propagating peak of population activity and the actual position of the moving stimulus increased with stimulus speeds. Data points show mean spatial lags for each speed and direction (bootstrap, $n=1{,}000$). *Blue squares* indicate centro-peripheral movement, red triangles indicate opposite motion direction. Latencies were calculated by linear regression. Latency for centro-peripheral motion was 42 ms, and 38 ms for peripheral-central direction (significance of direction difference: **=$p<0.00001$; *=$p<0.01$). (Modified from Jancke et al. ©2004b, by permission from Wiley-Blackwell) (*see Color Plates*)

led to a match between the peak of population activity and actual stimulus position as indicated by a spatial lag of nearly zero.

Spatial asymmetries for representations of moving objects (Mateeff and Hohnsbein 1988; Müsseler and Aschersleben 1998) might be the result of active mechanisms, compensating neural delays for one direction on the cost of delays in the opposite direction (Jensen and Martin 1980). Van Beers et al. (2001) proposed a number of putative mechanisms underlying differences in localization for foveopetal and foveofugal motion. These mechanisms include temporal asymmetries in neural delays, and a partial asymmetric spatial expansion of the retinal representation, both comparable to our findings. On the other hand, these authors provided evidence that when shifting gaze, the central nervous system is able to compensate for localization errors by sensor motor integration to maintain position constancy, maybe by taking advantage of these internally generated erroneous position signals.

Taken together we showed that in cat area 17 small moving squares of light could be represented as propagating peaks of activity across a "population receptive field" in which latencies for motion were significantly shorter than expected from the response to flash stimuli.

In terms of spike rates of single cell RFs, such behavior can be interpreted as dynamic and asymmetric enlargement of RF-sizes. As a consequence, RFs are shifted opposite to motion direction (Fu et al. 2004) causing neurons to respond with shorter delay times. Likewise, one might interpret such a shift as spatial phenomena: RF boundaries that were not responsive when mapped with flashed stimuli, become responsive when a stimulus moves, and RFs are therefore "pulled" towards an approaching moving stimulus (Pulgarin et al. 2003).

5.2.7 Motion Anticipation in Early Visual Cortex: A Novel Achievement in the Representation of Stimulus Position?

On the single cell level, neural latencies vary within a wide range of delay times. Generally, neurons that were sensitive to high stimulus speeds were found to have also short latencies for stationary light bars (Duysens et al. 1982). Comparing responses to flashed and moving slits of light, only few cells showed reduced latencies (Bishop et al. 1971). A stimulus dark edge evoked responses in advance of the discharge coming from the light edge (Bishop et al. 1971, 1973). Also, LGN neurons were found to respond with shorter delays to moving compared to flashed light bars (Orban et al. 1985). Part of these controversial findings may result from the relative wide bin sizes used for analyzing, which makes it difficult to detect small changes in latencies at the single cell level. Furthermore, the spatial-lag method is critically sensitive to response variability of single cells. The population approach used here however, transforms the various spatio-temporal dynamics of single cell activity into homogeneous activity patterns at the population level leading to a qualitative processing step from microscopic to mesoscopic levels (Freeman 2000; Dinse and Jancke 2001a). As a consequence, the population approach allows for

densely sampled and fine-scaled analysis of activity trajectories across a representative neural population.

Anticipatory mechanisms have also been reported for populations of retinal ganglion cells (Berry et al. 1999). The authors found that nonlinear contrast-gain control together with spatially extended receptive fields and a biphasic temporal response account for population activity that travels near the leading edge of a moving bar. Translating their data from millimeter retina into visual field coordinates (cf. DeVries and Baylor 1997; Hughes 1971), the retinal compensatory mechanisms were limited to stimulus speeds of approximately $5°s^{-1}$ which is in accordance with our result for peripheral-central motion direction. While we found a reduction of latencies in primary visual cortex up to $40°s^{-1}$, latencies for this range of speeds have not been investigated for the retina.

5.2.8 *Latency Differences May Contribute to the Flash-Lag Effect*

There is an extensive ongoing discussion about the nature of flash-lag effect, which has been studied under a large variety of experimental designs (Metzger 1932; MacKay 1958; Nijhawan 1994; Purushothaman et al. 1999; Krekelberg and Lappe 1999, 2001; Kirschfeld and Kammer 1999; Eagleman and Sejnowski 2000; Krekelberg et al. 2000; Sheth et al. 2000; Whitney et al. 2000). However, the neural substrates underlying this effect remain unknown.

The flash-lag effect has also been reported with no retinal motion indicating that extra-retinal information can be used to alternatively derive motion information (Schlag et al. 2000). Moreover, the flash-lag phenomenon not only applies to motion, but to other stimulus dimensions as well, such as color (Sheth et al. 2000). In any case, while not designed to mimic a particular psychophysical experiment – our experimental set-up corresponds to the traditional continuous motion protocol (Hazelhoff and Wiersma 1924) – the presented data revealed ~16 ms difference in latency between a flash and a moving stimulus corresponding to a 30% reduction in processing time. Reduced latencies of 10 ms for moving stimuli ($15°s^{-1}$) have recently been reported for neurons in primate V1 (Ceriatti et al. 2007). For the flash-lag effect described by Eagleman and Sejnowski (2000), the stimulus moved at $360°s^{-1}$ rotation angle leading to a displacement of about 5°, which translates into a delay of 14 ms, thus within the same range as found in our study. On the other hand, latency differences obtained in various paradigms commonly range between 40 and 80 ms (Krekelberg and Lappe 2001) most likely involving additional mechanisms of downstream cortical areas (but see next section). Furthermore, compensation of neural processing times is not restricted to the perceptual domain. It has recently been demonstrated that pointing movements towards the final position of a moving target were directed beyond its vanishing point suggesting that for goal-directed tasks, sensorimotor integration is critical for compensation of neural latencies (Kerzel and Gegenfurtner 2003).

Interestingly, a recent study investigated the flash-lag effect using two stimuli that moved towards the position of the flash. The authors hypothesized that two moving objects that would collide should "add their pre-activations" (Maiche et al. 2007). Indeed, it was found that such a stimulus configuration lead to even shorter latencies resulting in an increase of the flash-lag effect.

5.3 Neuronal Population Dynamics in Cortical Space

We hypothesized that pre-activation resulting from preceding stimulus displacements along the trajectory lead to an increased excitability, and thus to higher probabilities to fire action potentials when the stimulus moves across the PRF. Long-range horizontal connections may constitute a possible cortical substrate for such pre-activation as the spreading sub-threshold activity (Grinvald et al. 1994; Bringuier et al. 1999) extends far beyond the classical spiking RF (Allman et al. 1985; cf. Fig. 5.1a). However, extracellular recordings as shown in the previous paragraphs provide no information about the accompanying intracellular events (see chapter Fregnac et al. in this book). To identify those cortical mechanisms involved in motion processing, we employed voltage-sensitive dye (VSD) imaging (Cohen et al. 1978; Grinvald et al. 1984) that allows sensitive monitoring of the changes in membrane potential across neuronal populations with high spatial and temporal resolutions (Shoham et al. 1999).

5.3.1 Optical Imaging: Recording of Widespread Cortical Activity in Real-Time

VSD imaging makes use of a fluorescent dye that incorporates into neuronal membranes. Dependent on the depolarization of the membrane potential in which it is inserted, the dye changes its properties: the higher the change in voltage across the neuronal membrane the higher the amount of emitted fluorescence. These optical signals are then detected by a highly sensitive camera system (Grinvald and Hildesheim 2004).

5.3.2 Sub-threshold Preactivation by Long-Range Horizontal Connections

To visualize how motion trajectories are represented across the cortical surface, small squares were moved with different speeds (16, 32, 64°s^{-1}). Figure 5.5a depicts cortical VSD responses in cat area 18 evoked by small squares moving downwards in the visual field. In all cases, we observed an initial fast spread (white contour) that

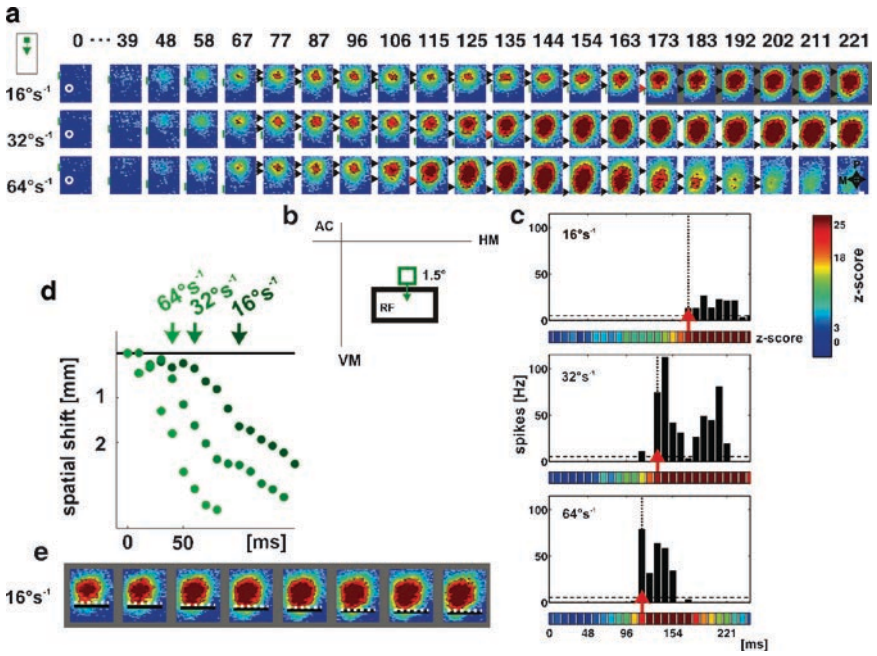

Fig. 5.5 Imaging cortical dynamics in response to moving squares. (**a**) Time courses of evoked cortical activity are shown in single frames (scale bar at *bottom right* 1 mm). Time after stimulus onset is indicated at the *top*. From *top to bottom row*: moving squares presented at different speeds, 16, 32, and 64°s^{-1}. *Green vertical lines* indicate the onset of stimuli and their estimated trajectory along posterior–anterior axis (M, medial; P, posterior). Extracellular recording (multi units) was performed simultaneously at the cortical location marked by *white circles* at frame zero (see (**b**) for receptive field (RF) of the recorded neurons. Spiking activity propagates with different speeds in anterior direction (*lower black arrows*). (**c**) To verify that the approaching wave front of VSD activity corresponds to spiking threshold, Post Stimulus Time Histograms (PSTHs) of spike events were derived. Horizontal stippled line depicts significance (z-score = 2, 30 repetitions). As the electrode was placed outside the retinotopic representation of the square's starting position, no spikes are evoked at the onset of motion, although the dye signal reports subthreshold spread of activity (*bottom row* shows actual z-score levels at the electrode position). Spikes are detected, however, as soon as activity reaches the spiking threshold at the position of the electrode (see *red arrows* in PSTH, and in **a**). With increasing stimulus speed, shifts in latency between the PSTHs can be seen because spiking level reached the electrode earlier for higher speeds. Thus squares moving at different speeds evoke consecutive spikes at a fixed electrode position. (**d**) Spatial shift of the wave front of spiking activity, slopes indicate speed of propagation across the cortex. Increasing hue of green depicts increasing stimulus speed. (**e**) Magnified section of imaging frames shown in (**a**), *upper row*. Note that the wave front of spiking activity (*white stippled lines*) closely matches the projected location of the stimulus (*black lines*) indicating "on-line" tracking of motion (see text). (Modified and reprinted by permission from Macmillan Publishers Ltd: Nature (Jancke et al. ©2004a) (*see Color Plates*)

was followed by emerging activity, which started to propagate a gradually drawn-out anterior in the direction of the induced motion (lower black arrows in Fig. 5.5a; green dots in d).

In order to detect regions that are activated at spiking levels we placed a single electrode at a given cortical position (white circles in 1st frames) and multi-unit recordings were performed simultaneously to VSD imaging in order to map the neurons' RF location in visual space. Subsequently, the start of the stimulus was positioned above the marked RF area (Fig. 5.5b). Moving the square evoked spikes as soon as the stimulus entered the RF. Dependent on stimulus speed however, significant spiking activity was detected at different times resulting in shifts of spiking response onset (Fig. 5c). Importantly, this procedure enabled to relate the amplitude of the dye signal directly to spiking threshold. As can be seen by the traces at the bottom of Fig. 5.5c, high levels of the dye signal (black contours in Fig. 5.5a) consistently reported the onset of spiking activity at different times for individual stimulus speeds (red arrows). Thus, the stimulus trajectories were characterized by asymmetrically propagating waves of spiking activity moving according to stimulus speeds (Fig. 5.5d).

Note that anterior to the spiking wave front, significant sub-threshold activity could be detected (white contours). We propose that such spreading activity may provide a basis for faster spiking as it pre-activates cortical areas ahead of the motion trajectory. Figure 5.5e depicts a larger scaled section of evoked activity in response to a square that was moved at $16°s^{-1}$ (compare Fig. 5.5, top row). The black bars mark the estimated center of the actual stimulus position projected onto the cortical coordinates (Albus 1975; Tusa et al. 1979). The white dotted lines show the cortical position of the propagating spiking wave front. As both lines closely match their position frame by frame, we observe an "on-line" tracking of a moving stimulus translating into ~50 ms reduction of latencies. For further increasing stimulus speeds however, spiking activity lagged behind stimulus projections.

Compared to area 17, cat area 18 seems to have more capacities in latency reduction, probably due to its preference for processing of higher temporal frequencies. On the other hand, if we consider the wave front (see transition from blue to green color in Fig. 5.3a, upper row; supplementary movie 1, and Fig. 5.2) instead of the peak of the population representations, full compensation of latencies could be claimed even for the PRF approach in area 17. At significant spiking wave front levels ($p < 0.01$, bootstrap) we calculated a spatial lag of nearly zero (0.006°) for a stimulus speed of $38°s^{-1}$. Thus depending on the read-out cortical mechanisms, different degrees of latency compensation could be achieved.

Note also that reduced latency does not occur instantaneously but needs time to build-up. Only when the stimulus trajectory has been established, continuative stimulation leads to the observed catch-up effect of the spiking wave front (Fig. 5.5a, upper row).

5.3.3 *Propagating Waves of Cortical Activity: The Line-Motion Illusion*

Almost a century ago, Gestalt psychologists (Wertheimer 1912; Kenkel 1913) made the striking observation that non-moving stimuli can give rise to motion

perception (Kanizsa 1951). Assuming that the facilitatory effect of the cue spread gradually in space and time (Posner et al. 1980; Sagi and Julesz 1986; Polat et al. 1998), the sensation of motion evoked by a subsequently flashed bar during the line-motion illusion could result from sequential suprathreshold activation, thus mimicking real motion drawing away from the local cue (Hikosaka et al. 1993; von Grünau et al. 1996a); Fig. 5.6a, b; see supplementary movie 2).

To explore cortical mechanisms underlying the "line-motion" illusion we examined, in cortical area 18 of the anaesthetized cat, responses to a flashed small square and a long bar alone, and the configuration of the line-motion illusion: a square briefly preceding the bar (Jancke et al. 2004a). Figure 5.6c depicts the cortical VSD response evoked by the small square alone. As the VSD signal is sensitive primarily to synaptic potentials rather than to spikes (Sterkin et al. 1999; Grinvald et al. 1999; Petersen et al. 2003), we searched here for an indirect way to delineate the spiking regions in the resulting optical maps (Albus 1975;

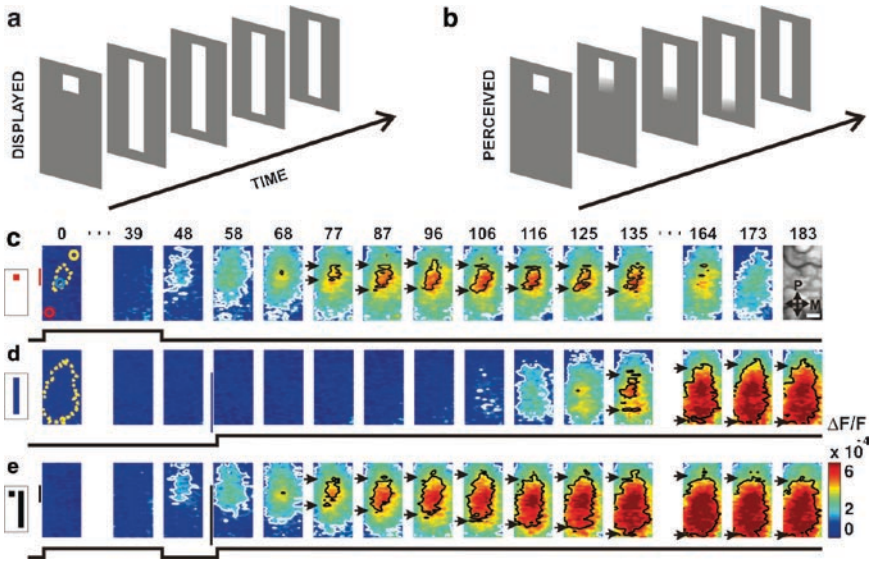

Fig. 5.6 Representations of stationary stimuli. (**a/b**) The line-motion paradigm. (**a**) Square ('cue') presented before a bar stimulus. (**b**) Subjects report illusory line-drawing (see supplementary movie 2). (**c**–**e**) Patterns of evoked cortical activity as a function of time. *Yellow dotted* contours approximate retinotopic representation of the stimuli; *coloured circles* indicate extracellular recording sites. *White contours* delimit low-amplitude activity (significance level; $p<0.05$). The cortical area imaged is shown at upper right. Scale bar, 1 mm; P, posterior; M, medial. *Vertical lines* indicate estimated position of the stimuli (sizes: 1.5° square, 1.5°×6° bar) along posterior-anterior axis. Time in milliseconds after stimulus onset is shown at the *top*. Stimulation period is depicted at the bottom of each row. Colour scale indicates averaged fractional changes in fluorescence intensity ($\Delta F/F$). Stimuli: (**c**) Flashed small square. (**d**) Flashed bar. (**e**) Line-motion paradigm. Average of 22 trials. (Modified and reprinted by permission from Macmillan Publishers Ltd: Nature (Jancke et al. ©2004a) *(see Color Plates)*

Tusa et al. 1979). As has been shown in the previous section, spiking regions should be located in the area of high VSD amplitudes. We therefore analyzed the dynamic behavior of evoked low- and high-amplitude activity separately. Again, low-amplitude activity spread far beyond the retinotopic representation of the square at ~0.09 ms^{-1}, consistent with conduction velocity along horizontal connections (white contour, Grinvald et al. 1994; Bringuier et al. 1999; Benucci et al. 2007). In contrast, high-amplitude activity (delimited by black contours) showed negligible lateral extension (Fig. 5.6c, arrows), after an initial ~20 ms period of spread. Single-unit recordings (colored circles; Fig. 5.6c, first frame) confirmed that spiking activity evoked by the square was limited to the high-amplitude area. The second stationary stimulus, the bar, flashed alone 60 ms later, yielded a similar finding (Fig. 5.6d). High-level activity delineated a circumscribed region representing the elongated shape of the bar almost at once (compare upper and lower black arrows).

Next, we investigated the spatio-temporal pattern of activity evoked by the line-motion paradigm (Fig. 5.6e). In contrast to the conditions in which either the square or the bar was flashed alone, the spike discharge zone did not remain stable but was gradually drawn out towards the end of the cortical bar representation (lower arrows). Thus, although these two stimuli were stationary, the anterior portion of the high-activity region propagated similarly to moving stimuli (Fig. 5.6a), suggesting, that cortical correlates of illusory line-motion were directly visualized here (see supplementary movie 3).

These findings demonstrate the effect of spatio-temporal patterns of sub-threshold synaptic potentials on cortical processing and the shaping of perception. While psychophysical studies also implicate top-down involvement of higher cortical areas (Hikosaka and Miyauchi 1993; von Grünau and Faubert 1994; Shimojo et al. 1997), others argue for essential bottom-up, i.e. stimulus induced mechanisms, occurring at early processing stages (Hikosaka et al. 1993; Steinman et al. 1995; von Grünau et al. 1996b).

We suggest that the characteristics of sub-threshold spread in early visual areas as shown here, are basic properties of the primary visual cortex involved in motion induction, and thus, cortical correlates of the bottom-up mechanism underlying the line-motion illusion without need of attention (Cavanagh et al. 1989, von Grünau et al. 1996b; Kawahara et al. 1996; Downing and Treisman 1997). It has been reported that when multiple inducers (or different stimulus features like color, contrast, or texture) are used there is evidence for a second top-down component that operates on a slower timescale (Hikosaka and Miyauchi 1993; von Grünau et al. 1996b; Nakayama and Mackeben 1989). Furthermore, the illusory line-motion can be modulated by attention (Downing and Treisman 1997), or can be voluntarily induced by non-retinotopic mechanisms (Hikosaka and Miyauchi 1993) even across sensory modalities (Shimojo et al. 1997, but see Downing and Treisman 1997). These top-down processing and attentional/attention seeking mechanisms remain to be explored in behaving subjects, by bringing together psychophysics and functional imaging.

5.4 Conclusions

Visual illusions such as the flash-lag and the line-motion illusions reveal discrepancies between the physically present world outside and internal *re*-presented sensation. What can we learn about the brain when studying such phenomena? Of course, the brain did not evolve its enormous complexity in order to deceive in every- day life. The task the visual system has to solve is to generate and interpret internally meaningful patterns of neuronal activity that enable successful interaction in natural environments. Visual illusions may therefore appear as artificial extremes of what the neuronal system has evolved to handle. The brain uses its tremendous flexibility - that still cannot be achieved by technical devices - in order to navigate and survive within rapidly changing visual input. In this framework, adaptation, stability that preserves flexibility, and prediction, are the essential capacities that have to be acquired throughout ongoing individual learning and evolutionary processes.

5.4.1 Anticipation and Integration: Important Capacities of the Brain

What are then advantages of producing far reaching sub-threshold waves of activities? Apart from well-documented context dependent lateral perceptual modulation (Polat and Sagi 1993; Polat et al. 1998), we believe that the spatio-temporal pattern of cortical activity waves is important in motion integration (Jancke 2000) and prediction. Any sudden appearing object (e.g. a prey, a predator – or a car nowadays) is potentially about to move (Dragoi et al. 2002). Sub-threshold cortical activity that spreads far ahead of the actual stimulus representation may therefore "prepare" the cortex for an object's putative trajectory. Such a strategy can save neuronal processing times. When actual movement occurs, neurons that represent position ahead of the stimulus are already close to the firing threshold and can react more rapidly to motion onset.

However, there is still a gap of knowledge about how timing information provided by visual cortical neurons map to perception (Seriès et al. 2002). Along the visual pathway various predictive (Nijhawan 1994; Rao and Ballard 1999) and integrative mechanisms (Krekelberg and Lappe 1999; Eagleman and Sejnowski 2000) starting from the retina (Berry et al. 1999) up to sensorimotor transformation (Kerzel and Gegenfurtner 2003) are involved in processing of motion. It remains an open question how the representation of moving stimuli in the primary visual cortex, in particular its reduced response latencies as reported here, contribute to the processing of object position in higher brain areas.

In summary we have showed that neuronal populations at the first cortical processing stage, the primary visual cortex, incorporate signatures of neuronal

motion initiation and anticipation. Once a stimulus continues to move, we demonstrated that sub-threshold cortical activity spreads ahead of retino-thalamic input leading to reduction of neuronal delay times as compared to a stationary flash. Depicting neuronal activity in stimulus space, we observed that reduced delay times cause shifts of RFs opposite to motion direction. This effect does not fully explain but may contribute to the well-known "flash-lag" phenomena: a moving and a flashed stimulus presented aligned, are perceived with spatial offset in which the moving stimulus appears ahead.

We suggest that preceding stimulation evoke pre-activation via long-range horizontal axons and increase the postsynaptic potential close to firing thresholds, thus preparing the ground for reduced latencies for subsequent stimuli. Such a cortical mechanism seems to be also involved in the line-motion phenomena, in which a bar, flashed at once after a small dot, is perceived as being gradually drawn-out. Here, illusory motion is seen despite stationary input, thus uncovering the underlying propagation of far spreading cortical activity.

Integration and boosting of propagating sub-threshold activity may therefore be a fundamental cortical mechanism for initiation of motion processing in response to spatially close and temporally successive visual input.

5.5 Supplementary Materials (CD-ROM)

Movie 1 Population representation of a moving square stimulus in cat area 17 (*file 5_M1_population.avi*). Representation of a moving square across the population receptive field (PRF). The PRF was derived from pooled activity of 178 neurons recorded in cat area 17. The RFs of all neurons densely cover a region along 2.8° in the central visual field (horizontal white line). Each neuron contributes to the overall activity distribution dependent on its relative RF location (see text). The white outlined square shows the stimulus (0.4°) as it moves across the visual field (speed = 38.4°s^{-1}). Spiking population activity forms a propagating peak that tracks the stimulus with a spatial lag due to neural delay times.

Movie 2 The line-motion stimulus (file *5_M2_linemotion.avi).* The line-motion illusion. The movie presents four different configurations of the line-motion illusion, consisting of pre-cueing small squares at four different positions followed by a stationary bar. Although the bar is presented at once, it is perceived as being drawn out from the position of the small squares.

Movie 3 V1 population response to the line motion (*file 5_M3_linemotionV1.avi).* Imaging cortical correlates of illusion in the visual cortex. Slow-motion video of the cortical representation of the line-motion paradigm in cat area 18 (posterior = top, medial = right, cf. Fig. 5.6e). Optically detected activity within 5.5 × 2.9 mm cortical surface is shown (sampling rate 9.6 ms, stimulus onset at frame zero). The first frames show a rapid spread of low amplitude activity (light blue, green, and yellow) followed by high-level activity (red) that gradually propagates towards the end of the cortical bar representation thus reporting motion. Blue vertical line

indicates estimated position and sizes of the stimuli along posterior-anterior axis (1.5° square, 6° bar; horizontal line approximates position along medial-lateral axis). Color bar indicates averaged fractional changes in fluorescence intensity ($\Delta F/F$, 22 trials). White contour delimit significance level, black contour encircles the spike discharge zone, see text).

Acknowledgments D.J. supported by Minerva Foundation, BMBF, Deutsche Forschungsgemeinschaft (Scho 336/4-2 and Di 334/5-1,3). F.C. supported by Marie Curie EU fellowship. A.G. supported by the Grodetsky Center, Goldsmith, Korber & ISF Foundations, BMBF/MOS, and NIH 1R01-EB00790-01 grants.

References

Albus K (1975) A quantitative study of the projection area of the central and the paracentral visual field in area 17 of the cat I. The precision of the topography. Exp Brain Res 24:159–179

Allman J, Miezin F, McGuiness E (1985) Stimulus specific responses from beyond the classical receptive field: neurophysiological mechanisms for local-global comparisons in visual neurons. Annu Rev Neurosci 8:407–430

Benucci A, Frazor RA, Carandini M (2007) Standing waves and traveling waves distinguish two circuits in visual cortex. Neuron 55:103–117

Berry MJ II, Brivanlou IH, Jordan TA, Meister M (1999) Anticipation of moving stimuli by the retina. Nature 398:334–338

Bishop PO, Coombs JS, Henry GH (1971) Responses to visual contours: Spatio-temporal aspects of excitation in the receptive fields of simple striate neurones. J Physiol (London) 219:625–657

Bishop PO, Coombs JS, Henry GH (1973) Receptive fields of simple cells in the cat striate cortex. J Physiol (London) 231:31–60

Bringuier V, Chavane F, Glaeser L, Frégnac Y (1999) Horizontal propagation of visual activity in the synaptic integration field of area 17 neurons. Science 283:695–699

Cavanagh P, Arguin M, von Grünau M (1989) Interattribute apparent motion. Vision Res 29:1197–1204

Ceriatti C, Botelho EP, Soares JGM, Gattass R, Fiorani M (2007) Shorter latencies to moving stimuli in primate V1 single units. Soc Neurosci Abstracts 37:279.22

Cohen LB, Salzberg BM, Grinvald A (1978) Optical methods for monitoring neuron activity. Annu Rev Neurosci 7:171–182

Dayan P, Abbott LF (2001) Theoretical neuroscience: computational and mathematical modeling of neural systems. Cambridge, MIT Press

DeVries SH, Baylor DA (1997) Mosaic arrangement of ganglion cell receptive fields in rabbit retina. J Neurophysiol 78:2048–2060

Dinse HR, Jancke D (2001a) Time-variant processing in V1: From microscopic (single cell) to mesoscopic (population) levels. Trends Neurosci 24:203–205

Dinse HR, Jancke D (2001b) Comparative population analysis of cortical representations in parametric spaces of visual field and skin: a unifying role for nonlinear interactions as a basis for active information processing across modalities. Prog Brain Res 130:155–173

Dragoi V, Sharma J, Miller EK, Sur M (2002) Dynamics of neuronal sensitivity in visual cortex and local feature discrimination. Nat Neurosci 5:883–891

Dumoulin SO, Wandell BA (2008) Population receptive field estimates in human visual cortex. Neuroimage 39:647–660

Downing PE, Treisman AM (1997) The line-motion illusion: Attention or impletion? J Exp Psychol Hum Percept Perform 23:768–779

Duysens J, Orban GA, Verbeke O (1982) Velocity sensitivity mechanisms in cat visual cortex. Exp Brain Res 45:285–294

Eagleman DM, Sejnowski TJ (2000) Motion integration and postdiction in visual awareness. Science 287:2036–2038

Fitzpatrick D (2000) Seeing beyond the receptive field in primary visual cortex. Curr Opin Neurobiol 10:438–443

Freeman WJ (2000) Mesoscopic neurodynamics: from neuron to brain. J Physiol (Paris) 94:303–322

Fu YX, Shen Y, Gao H, Dan Y (2004) Asymmetry in visual cortical circuits underlying motion-induced perceptual mislocalization. J Neurosci 24:2165–2171

Gegenfurtner KR, Hawken MJ (1996) Interaction of motion and color in the visual pathways. Trends Neurosci 19:394–400

Grinvald A, Anglister L, Freeman JA, Hildesheim R, Manker A (1984) Real-time optical imaging of naturally evoked electrical activity in intact frog brain. Nature 308:848–850

Grinvald A, Lieke E, Frostig R, Hildesheim R (1994) Cortical point-spread function and long-range lateral interactions revealed by real-time optical imaging of macaque monkey primary visual cortex. J Neurosci 14:2545–2568

Grinvald A, Shoham D, Shmuel A, Glaser D, Vanzetta I, Shtoyerman E, Slovin H, Arieli A (1999) In vivo optical imaging of cortical architecture and dynamics. In: Wind-Horst U, Johansson H (eds) Modern techniques in neuroscience research. Springer, New York, pp 893–969

Grinvald A, Hildesheim R (2004) VSDI: a new era in functional imaging of cortical dynamics. Nat Rev Neurosci 5:874–885

Hazelhoff FF, Wiersma H (1924) Die Wahrnehmungszeit [The sensation time]. Zeitschrift für Psychologie 96:171–188

Hikosaka O, Miyauchi S (1993) Voluntary and stimulus induced attention detected as motion sensation. Perception 22:517–526

Hikosaka O, Miyauchi S, Shimojo S (1993) Focal visual attention produces illusory temporal order and motion sensation. Vision Res 33:1219–1240

Hughes A (1971) Topographical relationships between the anatomy and physiology of the rabbit visual system. Doc Ophthalmol 30:33–159

Jancke D, Erlhagen W, Dinse HR, Akhavan AC, Giese M, Steinhage A, Schöner G (1999) Parametric population representation of retinal location: neuronal interaction dynamics in cat primary visual cortex. J Neurosci 19:9016–9028

Jancke D (2000). Orientation formed by a spot's trajectory: a two-dimensional population approach in primary visual cortex. J Neurosci 20 RC86:1–6

Jancke D, Chavane F, Naaman S, Grinvald A (2004a) Imaging correlates of visual illusion in early visual cortex. Nature 428:423–426

Jancke D, Erlhagen W, Schöner G, Dinse HR (2004b) Shorter latencies for motion trajectories than for flashes in population responses of primary visual cortex. J Physiol (London) 556:971–982

Jazayeri M, Movshon JA (2006) A new perceptual illusion reveals mechanisms of sensory decoding. Nat Neurosci 446:912–915

Jensen HJ, Martin J (1980) On localization of moving objects in the visual system of cats. Biol Cybern 36:173–177

Kanizsa G (1951). Sulla polarizzazione del movimento gamma. Archiva Psicologica Neurologica Psichiatrica 3:224–267

Kawahara J, Yokosawa K, Nishida S, Sato T (1996) Illusory line motion in visual search: attentional facilitation or apparent motion? Perception 25:901–920

Kenkel F (1913) Untersuchungen über den Zusammenhang zwischen Erscheinungsgröße und Erscheinungsbewegung bei einigen sogenannten optischen Täuschungen. Zeitschrift für Psychologie 67:358–449

Kerzel D, Gegenfurtner KR (2003) Neuronal processing delays are compensated in the sensorimotor branch of the visual system. Curr Biol 13:1975–1978

Kirschfeld K, Kammer T (1999) The Fröhlich effect: a consequence of the interaction of visual focal attention and metacontrast. Vision Res 39:3702–3709

Krekelberg B, Lappe M (1999) Temporal recruitment along the trajectory of moving objects and the perception of position. Vision Res 39:2669–2679
Krekelberg B, Lappe M, Whitney D, Cavanagh P, Eagleman DM, Sejnowski TJ (2000) The position of moving objects. Science 289:1107a
Krekelberg B, Lappe M (2001) Neuronal latencies and the position of moving objects. Trends Neurosci 24:335–339
MacKay DM (1958) Perceptual stability of a stroboscopically lit visual field containing self-luminous objects. Nature 181:507–508
Maiche A, Budelli R, Gomez-Sena L (2007) Spatial facilitation is involved in flash-lag effect. Vision Res 47:1655–1661
Mateeff S, Hohnsbein J (1988) Percepual latencies are shorter for motion towards the fovea than for motion away. Vision Res 28:711–719
Metzger W (1932) Versuch einer gemeinsamen Theorie der Phänomene Fröhlichs und Hazelhoffs und Kritik ihrer Verfahren zur Messung der Empfindungszeit. Psychologishe Forschung 16:176–200
Müsseler J, Aschersleben G (1998) Localizing the first position of a moving stimulus: The Fröhlich effect and an attention-shifting explanation. Percept Psychophys 60:683–695
Nakayama K, Mackeben M (1989) Sustained and transient components of focal visual attention. Vision Res 29:1631–1647
Nicolelis MA, Ghazanfar AA, Stambaugh CR, Oliveira LM, Laubach M, Chapin JK, Nelson RJ, Kaas JH (1998) Simultaneous encoding of tactile information by three primate cortical areas. Nat Neurosci 1:621–630
Nijhawan R (1994) Motion extrapolation in catching. Nature 370:256–257
Orban GA, Hoffmann KP, Duysens J (1985) Velocity selectivity in the cat visual system. I. Responses of LGN cells to moving bar stimuli: a comparison with cortical areas 17 and 18. J Neurophysiol 54:1026–1049
Petersen C, Grinvald A, Sakmann B (2003) Spatiotemporal dynamics of sensory responses in layer 2/3 of rat barrel cortex measured in vivo by voltage-sensitive dye imaging combined with whole-cell voltage recordings and neuron reconstructions. J Neurosci 23:1298–1309
Polat U, Sagi D (1993) Lateral interactions between spatial channels: suppression and facilitation revealed by lateral masking experiments. Vision Res 33:993–999
Polat U, Mizobe K, Pettet MW, Kasamatsu T, Norcia AM (1998) Collinear stimuli regulate visual responses depending on cell's contrast threshold. Nature 391:580–584
Posner MI, Snyder CRR, Davidson BJ (1980) Attention and the detection of signals. J Exp Psychol 109:160–174
Pulgarin M, Nevado A, Guo K, Robertson RG, Thiele A, Young MP (2003) Spatio-temporal regularities beyond the classical receptive field affect the information conveyed by the responses of V1 neurons. Soc Neurosci Abstracts 33:910.16
Purushothaman G, Patel SS, Bedell HE, Ogmen H (1999) Moving ahead through differential visual latency. Nature 396:424
Rao RPN, Ballard DH (1999) Predictive coding in the visual cortex: a functional interpretation of some extra-classical receptive field effects. Nat Neurosci 2:79–87
Sagi D, Julesz B (1986) Enhanced detection in the aperture of focal attention during simple discrimination tasks. Nature 321:693–695
Salinas E, Abbott LF (1994) Vector reconstruction from firing rates. J Comput Neurosci 1:89–107
Schlag J, Cai RH, Dorfman A, Mohempour A, Schlag-Rey M (2000) Extrapolating movement without retinal motion. Nature 403:38–39
Seriès P, Georges S, Lorenceau J, Frégnac Y (2002) Orientation dependent modulation of apparent speed: a model based on the dynamics of feed-forward and horizontal connectivity in V1 cortex. Vision Res 42:2781–2797
Sheth BR, Nijhawan R, Shimojo S (2000) Changing objects lead briefly flashed ones. Nat Neurosci 3:489–495

Shimojo S, Miyauchi S, Hikosaka O (1997) Visual motion sensation yielded by non-visually driven attention. Vision Res 37:1575–1580

Shoham D, Glaser DE, Arieli A, Kenet T, Wijnbergen C, Toledo Y, Hildesheim R, Grinvald A (1999) Imaging cortical dynamics at high spatial and temporal resolution with novel blue voltage-sensitive dyes. Neuron 24:791–802

Steinman BA, Steinman SB, Lehmkuhle S (1995) Visual attention mechanisms show a center-surround organization. Vision Res 35:1859–1869

Sterkin A, Arieli A, Ferster D, Glaser DE, Grinvald A (1999) Real time optical imaging in cat visual cortex exhibits high similarity to intracellular activity. Abstract of the 5th IBRO World Congress of Neuroscience, p 122

Szulborski RG, Palmer LA (1990) The two-dimensional spatial structure of nonlinear subunits in the RFs of complex cells. Vision Res 30:249–254

Tusa RJ, Rosenquist AC, Palmer LA (1979) Retinotopic organization of areas 18 and 19 in the cat. J Comp Neurol 185:657–678

van Beers RJ, Wolpert DM, Haggard P (2001) Sensorimotor integration compensates for visual localization errors during smooth pursuit eye movements. J Neurophysiol 85:1914–1922

Victor JD, Purpura K, Katz E, Mao B (1994) Population encoding of spatial frequency, orientation, and color in macaque V1. J Neurophysiol 72:2151–2166

von Grünau M, Faubert J (1994) Intra-attribute and interattribute motion induction. Perception 23:913–928

von Grünau M, Racette L, Kwas M (1996a) Measuring the attentional speed-up in the motion induction effect. Vision Res 36:2433–2446

von Grünau M, Dube S, Kwas M (1996b) Two contributions of motion induction: a preattentive effect and facilitation due to attentional capture. Vision Res 36:2447–2457

Wertheimer M (1912) Experimentelle Studien über das Sehen von Bewegung. Zeitschrift für Psychologie 61:161–265

Whitney D, Murakami I, Cavanagh P (2000) Illusory spatial offset of a flash relative to a moving stimulus is caused by differential latencies for moving and flashed stimuli. Vision Res 40:137–149